AIP | Journal of Applied Physics

The heterogeneous structure of metallic glasses revealed by superconducting transitions

B. Huang, H. Y. Bai, P. Wen, D. W. Ding, D. Q. Zhao et al.

Citation: J. Appl. Phys. **114**, 113508 (2013); doi: 10.1063/1.4822018
View online: http://dx.doi.org/10.1063/1.4822018
View Table of Contents: http://jap.aip.org/resource/1/JAPIAU/v114/i11
Published by the AIP Publishing LLC.

The heterogeneous structure of metallic glasses revealed by superconducting transitions

B. Huang, H. Y. Bai, P. Wen, D. W. Ding, D. Q. Zhao, M. X. Pan, and W. H. Wang[a)]
Institute of Physics, Chinese Academy of Sciences, Beijing 100190, People's Republic of China

(Received 2 September 2013; accepted 5 September 2013; published online 20 September 2013)

It has been postulated that metallic glasses, in contrast to their crystalline counterparts, exhibit nano-scale structural heterogeneity which is crucial for understanding the long-standing issues of relaxations and deformation of glasses. We fabricate micrometer scale metallic glassy fibers (MGFs) with different diameters and structural configurations, and find that the thinner MGFs cooled down with faster cooling rates have smaller superconducting transition temperatures and wider transition widths. We show that the superconducting properties correlate with the heterogeneous microstructure of metallic glasses and can be used as a novel way to experimentally characterize the structural heterogeneity of metallic glasses. © *2013 AIP Publishing LLC*.
[http://dx.doi.org/10.1063/1.4822018]

I. INTRODUCTION

Metallic glasses (MGs) synthesized through rapid quenching of supercooled liquids inherit the disordered structural features of liquids with a large amount of free volume.[1,2] It has been postulated that nano-scale heterogeneity could exist in MGs which plays a crucial role in the mechanical behavior,[3–5] relaxations[6,7] and glass transitions[8,9] of MGs. The wide distributions of energy dissipation and local indentation modulus in the nanometer scale implying the heterogeneous structure of MGs have been detected with atomic force microscopes (AFM)[10,11] and transmission electron microscopes (TEM)[4,5] in some MGs. Molecular dynamic simulations[12,13] and experimental phenomena[7,14,15] like mechanical hysteresis in dynamical micropillar tests and apparent β relaxation peaks in the dynamic mechanical spectroscopy (DMA) also indirectly demonstrate the heterogeneous structure with loosely bonded cores in MGs. However, it is still disputable that whether the loosely packed domains exist or not in MGs and how the heterogeneous structure affects the macroscopic properties of MGs. To our knowledge, little work has been done to explore the microstructure of MGs from their physical properties such as superconductivity, which is sensitive to microstructural characteristics.[16] It was reported that microstructure fluctuations can significantly influence the properties of superconductors in the vicinity of the transition temperatures.[17] Therefore, the superconductivity could provide us a new way to identify the heterogeneous structural features of glasses.

In this paper, we study the superconductivity changes of $La_{60}Cu_{20}Ni_{10}Al_{10}$ and $La_{65}Al_{10}Cu_{20}Co_5$ metallic glassy fibers (MGFs) upon the change of their diameters. We find thinner MGFs show smaller T_c and broader transition regions $\Delta T_c/T_c$. The deterioration of superconductivity is correlated with the electron density fluctuations and heterogeneous microstructure induced by different cooling rates. The difference of the superconductivity for the two types of MGFs is also discussed from their inhomogeneous structural features. Our experimental results may provide new evidence for the intrinsic heterogeneous microstructure of metallic glasses.

II. EXPERIMENTS

We used MGFs as model systems due to their diameter can be readily controlled in preparation, and the MGFs with different diameters have different cooling rates and then different structural configurations.[18] Therefore, we can study the correlation between the superconductivity and the structural features of MGs. $La_{60}Cu_{20}Ni_{10}Al_{10}$ and $La_{65}Al_{10}Cu_{20}Co_5$ MGFs with diameters in micrometer scale and lengths of more than 5 cm were manufactured with the method of drawing glassy rods in the supercooled liquid regions.[18] The glassy structure of the MGFs was confirmed by X-ray diffraction (XRD). The surface topography and size were detected with the scanning electron microscope (SEM). The superconductivity was studied through measuring the resistivity with the standard four-probe technique down to 1.8 K using the physical property measurement system (PPMS) 6000 of Quantum Design Company. The heat capacity near the glass transition temperatures (T_g) was measured under a purified argon atmosphere in a Perkin Elmer DSC-7. The dynamical mechanical behavior of $La_{60}Cu_{20}Ni_{10}Al_{10}$ and $La_{65}Al_{10}Cu_{20}Co_5$ metallic glassy ribbons with thickness at micrometer scale was tested on a TA Q800 dynamical mechanical analyzer.

III. RESULTS AND DISCUSSIONS

Figure 1(a) shows the SEM photographs of our fabricated $La_{60}Cu_{20}Ni_{10}Al_{10}$ and $La_{65}Al_{10}Cu_{20}Co_5$ MGFs. The geometry of the MGFs is successive and uniform. Their diameters range from several to tens of micron. Figure 1(b) shows the XRD patterns of the MGFs. The absence of sharp crystalline peaks indicates the fully amorphous structure. Figure 2(a) presents the resistivity ρ scaled by the normal resistivity ρ_0 for $La_{60}Cu_{20}Ni_{10}Al_{10}$ MGFs with different diameters at low temperatures and under a zero magnetic filed. ρ_0 is the resistivity at 3 K. ρ/ρ_0 of the MGFs falls down to zero

a)Author to whom correspondence should be addressed. Electronic mail: whw@iphy.ac.cn

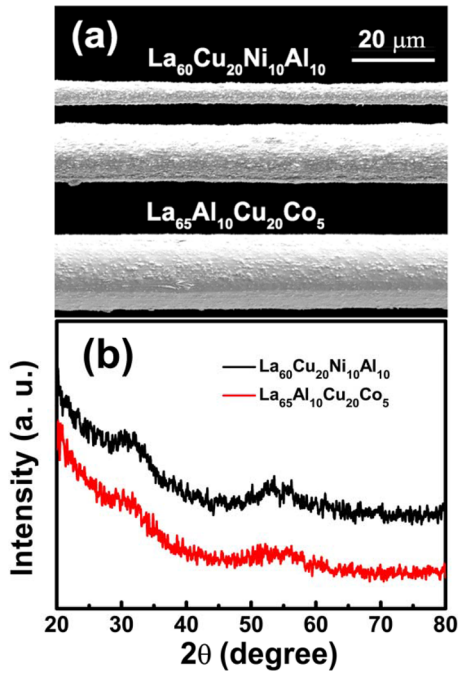

FIG. 1. (a) The SEM photographs for $La_{60}Cu_{20}Ni_{10}Al_{10}$ and $La_{65}Al_{10}Cu_{20}Co_5$ MGFs. (b) The XRD patterns of $La_{60}Cu_{20}Ni_{10}Al_{10}$ (the upper one) and $La_{65}Al_{10}Cu_{20}Co_5$ MGFs.

with temperatures decreasing which implies superconducting transitions. Both the temperatures, where ρ/ρ_0 deviates from the normal resistivity and reaches zero, decrease with the diameter decreasing. The superconducting transition temperature T_c is determined to be the temperature where ρ/ρ_0 reaches 0.5. From Fig. 2(a), one can see that the T_c of the MGF decreases with their diameter decreasing. The T_c of the MGF with a diameter of 15.0 μm is 2.43 K, while the T_c of the MGF with a diameter of 5.00 μm decreases to 2.13 K. The superconducting transition regions ΔT_c is the difference between the temperatures where ρ/ρ_0 are 0.1 and 0.9 [as indicated in Fig. 2(a)]. It can be clearly seen that the thinner MGFs have larger superconducting transition width $\Delta T_c/T_c$. The superconductivity of $La_{65}Al_{10}Cu_{20}Co_5$ MGFs shows similar behavior to that of $La_{60}Cu_{20}Ni_{10}Al_{10}$ MGFs (not shown here).

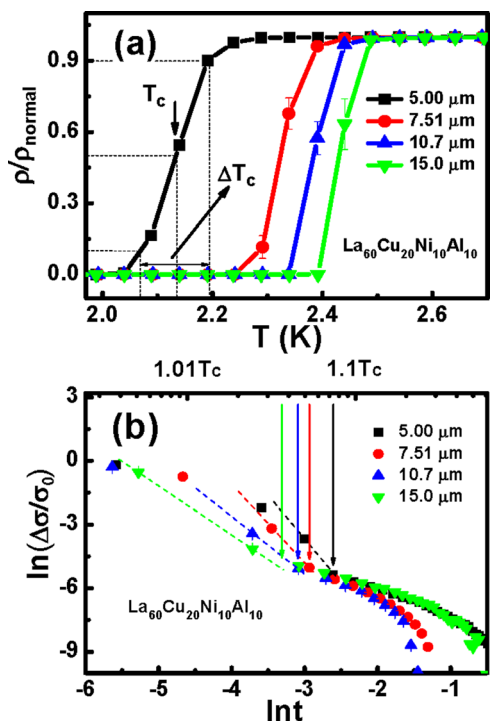

FIG. 2. (a) Temperature dependent scaled resistivity ρ/ρ_0 for $La_{60}Cu_{20}Ni_{10}Al_{10}$ MGFs with diameters of 5.00 μm, 7.5 μm, 10.7 μm, and 15.0 μm, respectively. (b) Excess conductivity $\Delta\sigma/\sigma_0$ versus the reduced temperature t in a logarithmic scale for $La_{60}Cu_{20}Ni_{10}Al_{10}$ MGFs with different diameters. The dashed lines are the guide for the eyes. The straight lines with arrows indicate the discontinuous points of $\Delta\sigma/\sigma_0$ at different temperatures scaled by T_c.

The size effects on the superconducting transitions should reflect structural characteristics of the MGFs. As the thin MGFs are formed from a melting liquid with a small volume of about 1 mm^3, the composition inhomogeneous is insignificant and cannot significantly influence the superconductivity. To avoid the influence of electric current densities, all the resistivity is measured in currents smaller than 10 μA. The coherence lengths of the studied MGFs should be several nanometers similar to those of amorphous LaAl alloys since the superconductivity of La-based MGs is mainly determined by La,[19,20] and the change of the superconductivity cannot be attributed to the modification of electron-phonon interactions by surfaces due to the much larger dimensions of the MGFs compared to the coherence lengths.[16] Therefore, the superconductivity change upon the diameter of the La-based MGFs can only be associated with their intrinsic structural characteristics.

To clearly exhibit the effects of structural fluctuations on the superconductivity, we plot the excess conductivity $\Delta\sigma/\sigma_0$ ($\Delta\sigma = \sigma - \sigma_0$) versus the reduced temperature t [$t = (T - T_c)/T_c$] in a logarithmic scale for $La_{60}Cu_{20}Ni_{10}Al_{10}$ MGFs in Fig. 2(b). The σ_0 is the normal conductivity at 3 K. The discontinuous change of $\Delta\sigma/\sigma_0$ near T_c ($t \lesssim 0.1$) can be attributed to sample structural inhomogeneity.[21] For thinner MGFs, the effect extends over a large temperature range implying the less homogeneous structure as predicted by the Ginzburg-Landau equation.[17] Actually, the superconducting transition widths $\Delta T_c/T_c$ can also reflect the structural heterogeneity,[22–24] which we will discuss in details later.

To show the structural evolution of MGFs with the diameter changing, we measure the heat capacity near glass transition temperature T_g of $La_{60}Cu_{20}Ni_{10}Al_{10}$ MGFs with different diameters using DSC. The DSC traces with obvious endothermic glass transition humps are shown in Fig. 3(a). The glass transition behavior varies when the diameter changes indicating different glassy states for these MGFs[25] as shown in the inset of Fig. 3(a). The cooling rates R_c for the MGFs can be roughly estimated as:[26] $R_c \approx 10/D^2$ (K/s), where D is the diameter of the MGF. As shown in Fig. 3(b), the T_g increases about 5 K when R_c increases one order of magnitude which is consistent with the glass transition theory.[27] This confirms that the MGFs with different diameters have different cooling rates and the thinner MGFs have fast cooling rates. The fictive temperature T_f represents the state of the glass and the change of T_f can characterize the variation of the glassy state.[28] We measured the T_f of the MGFs based on the DSC curves as shown Fig. 3(b). It can be seen that the T_f increases with

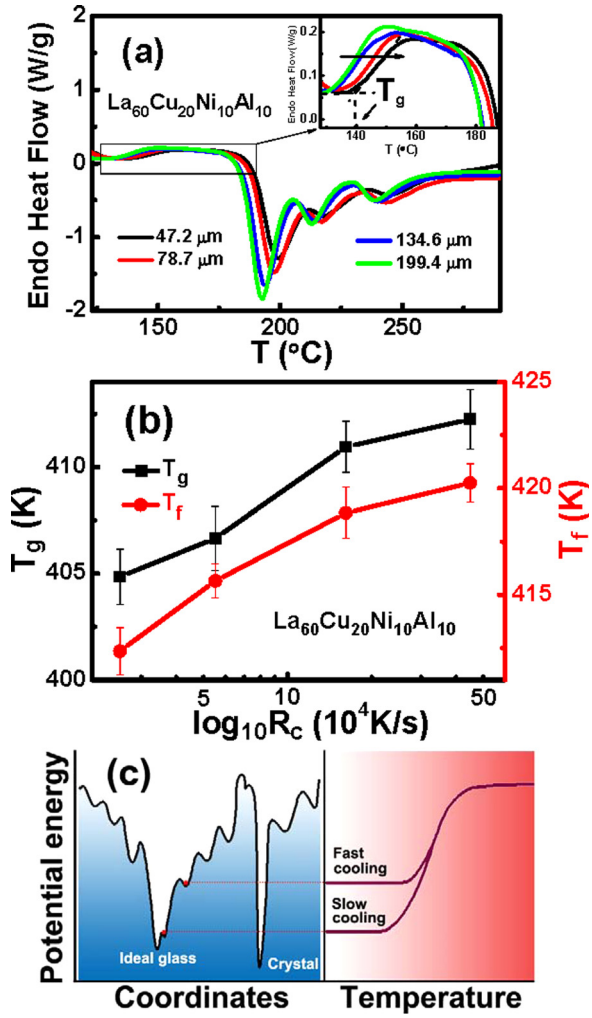

FIG. 3. (a) DSC traces for $La_{60}Cu_{20}Ni_{10}Al_{10}$ MGFs with different diameters. The inset shows the endothermic humps of glass transition for the MGFs. The horizontal arrow in the inset shows the moving direction of the DSC traces with the diameters decreasing. (b) Glass transition temperature T_g and fictive temperature T_f vs. cooling rate R_c for $La_{60}Cu_{20}Ni_{10}Al_{10}$ MGFs. (c) Schematic illustration of the solidification process of MGFs with the energy landscape. The left x-axis represents all configurational coordinates. The right x-axis represents temperature. The y-axis represents the total potential energy of the MG. Light blue and dark magenta represent high potential energy and temperatures, respectively.

decreasing diameters or increasing R_c. This indicates that the structure of thinner MGFs has more free volumes and more inhomogeneous structure.[29–31] The effect of the cooling rate on the structural configurations can be understood based on the energy landscape theory[30] as schematically illustrated in Fig. 3(c). By quenching from equilibrium liquid phases at a sufficiently high cooling rate (in the case of thinner MGFs), the system can be easily trapped into one of the basins with high potential energy, because the number of such basins is much more than that of basins with lower energy; when the cooling rate is considerably low (in the case of thick MGFs) but not as low as crystallization occurs, the system would fall into a basin with lower energy and a different structural configuration. Our results are also in accordance with recent simulations,[32] which show that glasses cooled down with faster cooling rates involve in relatively large clusters and more inhomogeneous structure.

The different structural configurations caused by different R_c are the main reason for the different superconductivity of the MGFs. Figure 4(a) shows the R_c dependent T_c for the La-based MGFs in a semilogarithmic scale. The T_c and R_c for bulk $La_{60}Cu_{20}Ni_{10}Al_{10}$ and $La_{65}Al_{10}Cu_{20}Co_5$ metallic glasses[33,34] are also plotted. One can see that the T_c deceases with the increase of R_c and the decrease is much faster for thinner MGFs with larger R_c. The T_c change trend of $La_{65}Al_{10}Cu_{20}Co_5$ MGFs is similar and the T_c are obviously larger compared with $La_{60}Cu_{20}Ni_{10}Al_{10}$ MGs. For $La_{60}Cu_{20}Ni_{10}Al_{10}$ MGs, the T_c decreases about 15% when R_c increases from 2.5×10^2 K/s to 4.0×10^7 K/s. For $La_{65}Al_{10}Cu_{20}Co_5$ MGs, the T_c decreases only about 3% when R_c increases from 2.5×10^2 K/s to 1.4×10^7 K/s. The T_c for $La_{60}Cu_{20}Ni_{10}Al_{10}$ is more sensitive to R_c than that of $La_{65}Al_{10}Cu_{20}Co_5$ MGFs as shown in Fig. 4(a).

For La-based MGs, in which La plays the dominant role for superconductivity, the electron-phonon interaction parameters λ is about 0.8 indicating a moderately coupling strength.[19,33] The T_c of the MGs can be expressed as[35]

$$T_c = \left(\frac{\Theta}{1.45}\right)\exp\left[-\frac{1.04(1+\lambda)}{\lambda-\mu^*(1+0.62\lambda)}\right], \quad (1)$$

where Θ and μ^* are the Debey temperature and electron-electron Coulomb pseudopotential, respectively. Anderson *et al.* proposed that the growth of μ^*, i.e., the effective Coulomb repulsion between cooper pair electrons induced by the less effective electron motion should be the main reason for the degradation of T_c in a strongly disordered metal.[36] For the MGs fabricated with faster cooling rates and high concentrations of free volume, their electrons should

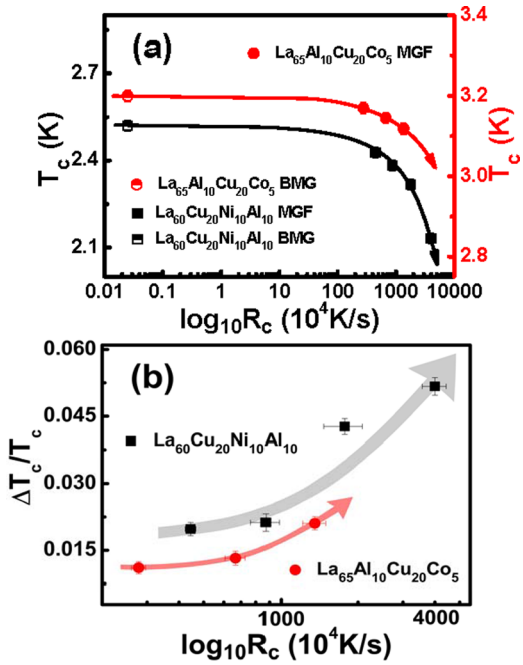

FIG. 4. (a) R_c dependent T_c for $La_{60}Cu_{20}Ni_{10}Al_{10}$ and $La_{65}Al_{10}Cu_{20}Co_5$ MGFs and their bulk MG form in a semilogarithmic scale. The curves with arrows are the guide for the eyes. (b) $\Delta T_c/T_c$ vs. R_c for $La_{60}Cu_{20}Ni_{10}Al_{10}$ and $La_{65}Al_{10}Cu_{20}Co_5$ MGFs in a semilogarithmic scale. The curves with arrows are the guide for the eyes.

diffuse slower and μ^* are larger due to the more inhomogeneous structure and higher electron density fluctuations. As a result, the T_c of these MGs decrease with the increase of R_c. Experiments and simulations have confirmed that the densities of states at Fermi level $N(E_F)$ are mainly responsible for the variation of T_c for series of MGs including La-based MGs when the compositions are changed.[19,37] The larger T_c for $La_{65}Al_{10}Cu_{20}Co_5$ MGFs compared with that of $La_{60}Cu_{20}Ni_{10}Al_{10}$ MGFs can be plausibly explained with its larger $N(E_F)$ associated with the nearest La-La separation.

Large superconducting transition widths $\Delta T_c/T_c$ are also closely associated with the inhomogeneous structure of superconductors.[22–24] We plot the $\Delta T_c/T_c$ versus R_c for the La-based MGFs in a semilogarithmic scale in Fig. 4(b). The thinner MGFs with larger R_c have larger $\Delta T_c/T_c$ for the two types of the MGFs. Considering cooling rate gradient between the surface and the center of a MGF, the thinner MGFs seem to have less inhomogeneous macrostructure than thicker ones. So, the increase of $\Delta T_c/T_c$ cannot be explained with macroscopic inhomogeneity, but can only be attributed to the more inhomogeneous microstructure caused by faster cooling rates. In the characteristic volume at the scale of superconducting coherence lengths, the fluctuations of La concentrations or atomic densities induced by the variation of effective hydrostatic pressure can lead to the broadening of superconducting transition widths of La-based MGs.[21] Larger structural fluctuations in nanosized regions caused by faster cooling rates lead to the increase of $\Delta T_c/T_c$ for thinner MGFs considering the nanoscale superconducting coherence lengths for La-based MGs.[19,20] Therefore, the depression of T_c and broadening of $\Delta T_c/T_c$ for La-based MGs fabricated with faster cooling rates imply the larger structural fluctuations associated with nanoscale structural heterogeneities at the scale of several nanometers. The characteristic lengths of the heterogeneities are in good agreement with those of flow units or shear transformation zones in MGs.[38,39]

We analyze the difference of the microstructure for $La_{60}Cu_{20}Ni_{10}Al_{10}$ and $La_{65}Al_{10}Cu_{20}Co_5$ MGFs through comparing their superconductivity. As shown in Fig. 3(b), the degradation of T_c is more pronounced and becomes quicker with R_c increasing for $La_{60}Cu_{20}Ni_{10}Al_{10}$ MGFs. As shown in Fig. 4(b), the $\Delta T_c/T_c$ of $La_{60}Cu_{20}Ni_{10}Al_{10}$ MGFs is larger than those of $La_{65}Al_{10}Cu_{20}Co_5$ MGFs even their values of R_c are similar, and the $\Delta T_c/T_c$ increases quickly with faster cooling rates for $La_{60}Cu_{20}Ni_{10}Al_{10}$ MGFs. The difference in the superconductivity manifests that $La_{60}Cu_{20}Ni_{10}Al_{10}$ MG could contain more free volume and its microstructure could be more heterogeneous than that of $La_{65}Al_{10}Cu_{20}Co_5$ MG. Figure 5 shows the temperature dependent loss modulus for $La_{60}Cu_{20}Ni_{10}Al_{10}$ and $La_{65}Al_{10}Cu_{20}Co_5$ MGs measured at 4 Hz. The T_g for the two MGs are 356 K and 387 K, respectively. The more pronounced β relaxation peak for $La_{60}Cu_{20}Ni_{10}Al_{10}$ MG as shown in Fig. 5 indicates more heterogeneous structure of this MG, because the degree of the heterogeneous structure is found to be proportional to the intensity of the β relaxation peak.[15,40] Therefore, the differences in T_c and $\Delta T_c/T_c$ for the two types of La-based MGs further confirm the correlation between the superconductivity and intrinsic heterogeneous microstructure in MGs, and the superconductivity can be used as a way to identify and characterize the structural inhomogeneity of MGs.

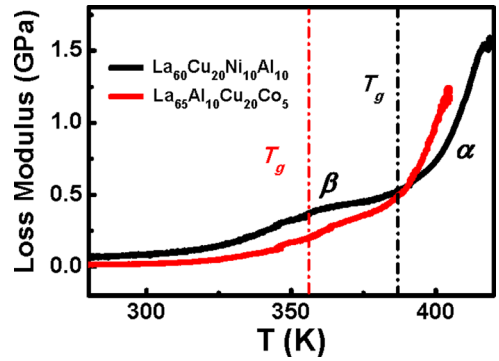

FIG. 5. Temperature dependent loss modulus for $La_{60}Cu_{20}Ni_{10}Al_{10}$ and $La_{65}Al_{10}Cu_{20}Co_5$ MGs. The dashed-dotted lines at 356 K and 387 K mark the positions of T_g for $La_{60}Cu_{20}Ni_{10}Al_{10}$ and $La_{65}Al_{10}Cu_{20}Co_5$ MGs, respectively. The $La_{60}Cu_{20}Ni_{10}Al_{10}$ shows a pronounced β relaxation peak.

IV. CONCLUSIONS

We show that the superconductivity of the metallic glasses can reflect their different microstructural heterogeneities at the nanometer scale. The deterioration of the superconductivity is correlated with the more heterogeneous microstructure in superconducting metallic glasses, and some properties such as the superconductivity can be used to characterize the structural heterogeneity of metallic glasses. Our results could have implications for understanding the disordered structure and superconducting properties of metallic glasses.

ACKNOWLEDGMENTS

The authors are grateful for the experimental assistance and helpful discussions of S. K. Su, J. Ma, and Z. G. Zhu. The financial support of the NSF of China (Grant Nos. 51271195 and 51171204) and MOST 973 of China (Nr. 2010CB731603) is appreciated.

[1]H. S. Chen, Rep. Prog. Phys. **43**, 353 (1980).
[2]D. Turnbull and M. H. Cohen, J. Chem. Phys. **34**, 120 (1961).
[3]Y. F. Shi and M. L. Falk, Phys. Rev. Lett. **95**, 095502 (2005).
[4]Y. H. Liu, G. Wang, R. J. Wang, D. Q. Zhao, M. X. Pan, and W. H. Wang, Science **315**, 1385 (2007).
[5]H. B. Yu, X. Shen, Z. Wang, L. Gu, W. H. Wang, and H. Y. Bai, Phys. Rev. Lett. **108**, 015504 (2012).
[6]W. Dmowski, T. Iwashita, C.-P. Chuang, J. Almer, and T. Egami, Phys. Rev. Lett. **105**, 205502 (2010).
[7]L. S. Huo, J. F. Zeng, W. H. Wang, C. T. Liu, and Y. Yang, Acta Mater. **61**, 4329 (2013).
[8]T. Egami, S. Poon, Z. Zhang, and V. Keppens, Phys. Rev. B **76**, 024203 (2007).
[9]H. Tanaka, T. Kawasaki, H. Shintani, and K. Watanabe, Nature Mater. **9**, 324 (2010).
[10]Y. H. Liu, D. Wang, K. Nakajima, W. Zhang, A. Hirata, T. Nishi, A. Inoue, and M. W. Chen, Phys. Rev. Lett. **106**, 125504 (2011).
[11]H. Wagner, D. Bedorf, S. Küchemann, M. Schwabe, B. Zhang, W. Arnold, and K. Samwer, Nature Mater. **10**, 439 (2011).
[12]Y. Q. Cheng, A. J. Cao, and E. Ma, Acta Mater. **57**, 3253 (2009).

[13]T. Fujita, Z. Wang, Y. H. Liu, H. Sheng, W. H. Wang, and M. W. Chen, Acta Mater. **60**, 3741 (2012).
[14]J. C. Ye, J. Lu, C. T. Liu, Q. Wang, and Y. Yang, Nature Mater. **9**, 619 (2010).
[15]Z. Wang, P. Wen, L. S. Huo, H. Y. Bai, and W. H. Wang, Appl. Phys. Lett. **101**, 121906 (2012).
[16]M. Tinkham, *Introduction to Superconductivity*, 2nd ed. (McGraw-Hill, Singapore, 1996).
[17]A. Larkin and A. Varlamov, *Theory of Fluctuations in Superconductors*. (Clarendon Press, Oxford, 2009).
[18]J. Yi, X. X. Xia, D. Q. Zhao, M. X. Pan, H. Y. Bai, and W. H. Wang, Adv. Eng. Mater. **12**, 1117 (2010).
[19]K. Agyeman, R. Müller, and C. C. Tsuei, Phys. Rev. B **19**, 193 (1979).
[20]W. H. Wang, Nature Mater. **11**, 275 (2012).
[21]W. L. Johnson and C. C. Tsuei, Phys. Rev. B **13**, 4827 (1976).
[22]T. Watanabe, K. Obara, T. Ogushi, T. Numata, and T. Anayama, Appl. Phys. Lett. **39**, 113 (1981).
[23]G. Zwicknagl and J. Wilkins, Phys. Rev. Lett. **53**, 1276 (1984).
[24]A. Nordström, U. Dahlborg, and Ö. Rapp, Phys. Rev. B **48**, 12866 (1993).
[25]C. A. Angell, Science **267**, 1924 (1995).
[26]X. H. Lin and W. L. Johnson, J. Appl. Phys. **78**, 6514 (1995).
[27]M. D. Ediger, C. A. Angell, and S. R. Nagel, J. Phys. Chem. **100**, 13200 (1996).
[28]I. M. Hodge and A. R. Berens, Macromolecules **15**, 762 (1982).
[29]I. M. Hodge and G. S. Huvard, Macromolecules **16**, 371 (1983).
[30]P. G. Debenedetti and F. H. Stillinger, Nature **410**, 259 (2001).
[31]A. Slipenyuk and J. Eckert, Scr. Mater. **50**, 39 (2004).
[32]S. Singh, M. D. Ediger, and J. J. de Pablo, Nature Mater. **12**, 139 (2013).
[33]M. B. Tang, H. Y. Bai, M. X. Pan, D. Q. Zhao, and W. H. Wang, J. Non-Cryst. Solids **351**, 2572 (2005).
[34]M. B. Tang, H. Y. Bai, and W. H. Wang, Phys. Rev. B **75**, 172201 (2007).
[35]W. L. McMillan, Phys. Rev. **167**, 331 (1968).
[36]P. W. Anderson, K. Muttalib, and T. Ramakrishnan, Phys. Rev. B **28**, 117 (1983).
[37]M. Tenhover and W. L. Johnson, Phys. Rev. B **27**, 1610 (1983).
[38]D. Pan, A. Inoue, T. Sakurai, and M. W. Chen, Proc. Natl. Acad. Sci. U.S.A. **105**, 14769 (2008).
[39]S. T. Liu, Z. Wang, H. L. Peng, H. B. Yu, and W. H. Wang, Scr. Mater. **67**, 9 (2012).
[40]W. B. Jiang, P. Cui, Q. P. Kong, Y. Shi, and M. Winning, Phys. Rev. B **72**, 174118 (2005).